Original Article

Prognostic role of tertiary lymphatic structures and their modulation by adjuvant FOLFOX in stage III colon cancer: a retrospective cohort study

Chuang Zhang[1], Shao-Ke Wang[1], Nan Zun Teo[2], Matthew Yuan-Kun Wei[3], Hiroki Hashida[4], Chen-Feng Yu[1], Yan-Long Liu[1], Bin-Bin Cui[1]

[1]Department of Colorectal Surgery, Harbin Medical University Cancer Hospital, Harbin, China; [2]Department of General Surgery, Changi General Hospital, Singapore, Singapore; [3]Department of Surgery, University of Melbourne, Melbourne, Australia; [4]Department of Surgery, Hanwa Memorial Hospital, Osaka, Japan

Contributions: (I) Conception and design: C Zhang, YL Liu, BB Cui; (II) Administrative support: YL Liu, BB Cui; (III) Provision of study materials or patients: SK Wang; (IV) Collection and assembly of data: CF Yu; (V) Data analysis and interpretation: C Zhang; (VI) Manuscript writing: All authors; (VII) Final approval of manuscript: All authors.

Correspondence to: Yan-Long Liu, MD; Bin-Bin Cui, MD. Department of Colorectal Surgery, Harbin Medical University Cancer Hospital, No. 150 Haping Road, Nangang District, Harbin 150081, China. Email: liuyanlong@hrbmu.edu.cn; binbincui@hrbmu.edu.cn.

Background: Stage III colon cancer (CC) presents a critical therapeutic challenge due to its high recurrence risk. Identifying robust prognostic biomarkers to guide adjuvant therapy decisions is urgently needed in clinical practice. Tertiary lymphoid structures (TLSs), as immune aggregates within the tumor microenvironment, have emerged as potential indicators of immunological activity and treatment response. The objective of this study is to evaluate the role of TLSs in stage III CC, focusing on their potential as prognostic markers and their influence on patient outcomes, particularly in relation to chemotherapy response.

Methods: This retrospective cohort study enrolled 613 patients with pathologically confirmed stage III CC from two cohorts: 374 from Harbin Medical University and 239 from The Cancer Genome Atlas Colon Adenocarcinoma (TCGA-COAD) external validation cohort. Overall survival (OS) was the primary outcome, with a median follow-up period of 62 months. TLSs were assessed via immunohistochemistry and categorized by density and location [intratumoral (T score), peritumoral (P score)]. Prognostic significance was evaluated using multivariate Cox regression. A murine model was used to assess the immunomodulatory effects of folinic acid, oxaliplatin, and 5-fluorouracil (FOLFOX) chemotherapy on TLS formation.

Results: TLSs were present in 54.0% and 50.2% of patients in Cohorts 1 and 2, respectively. TLSs enriched with $CD8^+$ T cells and $CD20^+$ B cells were associated with improved OS. Multivariate analysis identified TLS presence as an independent predictor of better survival [hazard ratio (HR) =0.256, 95% confidence interval (CI): 0.093–0.707; P=0.009]. Higher intratumoral TLS density (T score) correlated with lower mortality risk (T2 *vs.* T0: HR =0.173, P=0.003), whereas higher peritumoral TLS density (P3) predicted worse prognosis (HR =5.887, P=0.04). *In vivo* experiments confirmed that FOLFOX treatment enhanced TLS formation and increased infiltration of immune cells including B cells, $CD4^+$/$CD8^+$ T cells, and dendritic cells.

Conclusions: TLSs serve as a reliable, independent prognostic biomarker in stage III CC. Their spatial distribution carries distinct prognostic implications, and FOLFOX-induced TLS formation suggests a dual role in cytotoxicity and immune activation. Incorporating TLS assessment into clinical workflows may improve risk stratification and guide personalized treatment, especially in designing immunochemotherapy strategies.

Keywords: Stage III colon cancer (stage III CC); tertiary lymphatic structure (TLS); tumor immune microenvironment (TIME); folinic acid, oxaliplatin, and 5-fluorouracil treatment (FOLFOX treatment); prognosis

Submitted Mar 07, 2025. Accepted for publication Apr 24, 2025. Published online Apr 27, 2025.
doi: 10.21037/jgo-2025-181
View this article at: https://dx.doi.org/10.21037/jgo-2025-181

Introduction

Colon cancer (CC) is one of the leading cause of cancer-related morbidity and mortality worldwide (1,2). The etiology of CC is complex and involves genetic, environmental, and lifestyle factors (2-4). Stage III CC is characterized by regional lymph node involvement and represents a critical point for therapeutic intervention. Multimodal treatment strategies, including adjuvant chemotherapy, are typically required to improve overall survival (OS) (5). Currently, the combination regimen of folinic acid, oxaliplatin, and 5-fluorouracil (FOLFOX) has become the standard adjuvant therapy for stage III patients and has been shown to significantly improve survival outcomes (6-8).

Prognostic evaluation in CC has traditionally relied on the Tumor-Node-Metastasis (TNM) staging system, which is widely used to guide treatment decisions in stage III patients. However, studies have shown that patients with the same stage may experience markedly different survival outcomes, with 5-year OS in stage III cases ranging from 15% to 75% (9-11). This highlights the limitations of TNM staging in individualized risk prediction. Although conventional pathological parameters—such as tumor differentiation, location, carcinoembryonic antigen (CEA) levels, and vascular or perineural invasion (VELIPI)—can assist in outcome estimation, their predictive accuracy for chemotherapy response remains limited (12). Therefore, there is an urgent need for more robust and sensitive biomarkers to refine risk stratification.

In recent years, increasing attention has been paid to the role of the immune microenvironment in CC prognosis. Tumor-infiltrating lymphocytes (TILs), particularly tertiary lymphoid structures (TLSs), have emerged as important prognostic indicators (13). A retrospective analysis by Saberzadeh-Ardestani *et al.* (14), based on 1,532 patients from the NCCTG N0147 trial who received standard FOLFOX with or without cetuximab, demonstrated that the prognostic value of TILs was dependent on tumor sidedness. In right-sided CC, low TIL density was associated with a twofold increase in the 5-year recurrence risk compared to high TILs, whereas in left-sided tumors, the increase was only about 30%. This suggests a significant interaction between TILs and tumor location (P=0.045).

TLSs, ectopic lymphoid aggregates resembling secondary lymphoid organs, have recently been recognized as potential immune biomarkers for predicting chemotherapy response (15-17). By promoting antigen presentation and immune cell recruitment, TLSs enhance anti-tumor immunity and may improve the efficacy of chemotherapy and immunotherapy (18-20). A study has shown that patients with higher TLS density exhibit better survival outcomes following chemotherapy (21). However, the precise role of TLSs in modulating the response to FOLFOX in stage III CC remains unclear. TLS formation is influenced by multiple factors, including tumor molecular subtype, immune microenvironment, and host immune

Highlight box

Key findings

- This study showed that tertiary lymphoid structures (TLSs) are critical components of the tumor immune microenvironment in stage III colon cancer (CC). TLSs, particularly those located intratumorally, were found to be associated with improved overall survival (OS).
- The study also showed that folinic acid, oxaliplatin, and 5-fluorouracil (FOLFOX) chemotherapy promotes TLS formation and immune cell infiltration, suggesting a synergistic relationship between chemotherapy and immune response modulation.

What is known and what is new?

- TLSs have been identified as prognostic markers in various cancers, including colorectal cancer, with their presence linked to patient outcomes.
- This study developed a spatial scoring system for TLSs in stage III CC, showing that higher intratumoral (T) scores correlate with better survival, while higher peritumoral (P) scores are linked to worse outcomes. It also demonstrates for the first time that FOLFOX chemotherapy enhances TLS formation, suggesting new combined chemotherapy and immunotherapy strategies.

What is the implication, and what should change now?

- These findings emphasize the importance of incorporating TLS evaluation into the prognosis and personalized treatment of stage III CC, potentially improving outcome predictions.
- Future strategies should focus on TLS-targeted approaches combining chemotherapy with immunotherapy. Further research is needed to refine TLS quantification and validate these strategies in clinical trials.

status (22). Although the immunological role of TLSs is increasingly appreciated, their prognostic and predictive value in the context of adjuvant therapy for stage III CC remains insufficiently studied. Considering that treatment response in CC is influenced by a multitude of factors, TLSs—as representative immune structures—may provide functional insights beyond those offered by traditional biomarkers, particularly in microsatellite-stable (MSS) or immune-cold tumors. This study aims to evaluate the prognostic significance of TLSs in stage III CC and to explore their potential as predictive biomarkers for response to FOLFOX, thereby contributing to the optimization of adjuvant therapy in this patient population. We present this article in accordance with the ARRIVE and STROBE reporting checklists (available at https://jgo.amegroups.com/article/view/10.21037/jgo-2025-181/rc).

Methods

Study design

This study integrated clinical analysis, histopathological evaluation, and animal experiments to investigate the prognostic significance of TLSs in stage III CC and their modulation by FOLFOX chemotherapy. First, a retrospective cohort of 613 patients from Harbin Medical University and The Cancer Genome Atlas Colon Adenocarcinoma (TCGA-COAD) was used to assess the association between TLS characteristics (density, location, composition) and OS via immunohistochemistry (IHC). Second, a spatial scoring system (T score and P score) was developed to quantify TLS distribution and evaluate its prognostic value. Third, a murine MC38 CC model was used to examine the effect of FOLFOX on TLS formation and immune cell infiltration, aiming to validate the immunomodulatory potential of chemotherapy. This multi-step approach aimed to link TLS features with clinical outcomes and explore underlying mechanisms. A protocol was prepared before the study without registration.

Study populations

The study included two independent cohorts of stage III CC patients. The Harbin Medical University cohort comprised 374 stage III CC patients (Cohort 1), who underwent surgical resection at the Harbin Medical University Cancer Hospital (Harbin, China) between January 2016 and January 2018. TCGA-COAD external validation cohort comprised 239 stage III CC patients (Cohort 2), whose clinical and genomic data were downloaded from the University of California, Santa Cruz Xena (UCSC-Xena) database (https://xenabrowser.net/datapages/). The primary endpoint of the study was OS, which was defined as the time from the date of surgery to the date of death or last follow-up. All patients had pathologically confirmed stage III CC and underwent radical resection without prior treatment with molecular targeted therapies or immunotherapy. To be eligible for inclusion in the study, the patients had to meet the following inclusion criteria: (I) have pathologically confirmed stage III CC with lymph node involvement; (II) have complete clinicopathological and follow-up data, including OS information; (III) have tissue samples available for research analysis. Patients were excluded from the study if they met any of the following exclusion criteria: (I) had distant metastasis (stage IV CC) at diagnosis; (II) had a previous history of other malignancies or concurrent malignancies; (III) had incomplete follow-up or missing clinical data; and/or (IV) had poor quality or insufficient tissue samples for reliable analysis.

As a retrospective cohort study, no formal sample size calculation was conducted. However, post hoc power analysis based on OS confirmed that the sample of 613 patients was adequate to detect significant intergroup differences. Patients in Cohort 1 were followed every 3–6 months in the first 2 years and every 6–12 months thereafter via clinic visits, phone calls, or medical record review. Survival status was confirmed through documentation or contact with patients or families. The median follow-up was 62 months. This study was conducted in accordance with Declaration of Helsinki and its subsequent amendments, and was approved by the Ethics Committee of the Harbin Medical University Cancer Hospital (approval No. HMUIRB2024014). Written informed consent was obtained from all participants.

Evaluation of TLS

Tissue samples from all 374 patients in Cohort 1 were formalin-fixed and embedded in paraffin (FFPE). Serial sections (4 μm thick) of these tissues were used for hematoxylin and eosin (H&E) staining and IHC (23,24). IHC was performed to assess lymphocyte organization in the CC tissues, using antibodies against cluster of differentiation (CD)20 (Cat#ab64088, Abcam, 1:100, UK) (B cells), CD21 (Cat#ab315160, Abcam, 1:50, UK) [dendritic cells (DCs)], CD8 (Cat#ab237709, Abcam)

(cytotoxic T cells), CD4 (Cat#ab133616, Abcam, 1:500, UK) (helper T cells), and CD23 (Cat#ab92495, Abcam, 1:400, UK) [follicular dendritic cells (FDCs)]. Each slide was reviewed for the presence and localization of TLSs by three independent observers. Additionally, the number of tumor-infiltrating immune cells outside the TLSs was quantified.

Multispectral fluorescent IHC

To further analyze the immune cell populations in the TLSs, multispectral immunohistochemistry (mIHC) staining (25) was performed on the FFPE tissue sections showing TLS presence as per the instructions of the Opal Color Kit (Cat#NEL871001KT, Akoya Biosciences, 1:100, USA). This method was used to identify key adaptive immune cells, including $CD4^+$ T cells, $CD8^+$ T cells, $CD20^+$ B cells, $CD21^+$ DCs, and $CD23^+$ FDCs. Multiple-color slides were imaged using a PerkinElmer Vectra automated multispectral microscope (PerkinElmer, Hopkinton, MA, USA), and the images were analyzed using PerkinElmer inForm analysis software.

TLS scoring system and prognostic model

TLSs were categorized based on their maturation stages, which include lymphocyte aggregates and lymphocyte follicles. The lymphocyte follicles were further classified into those with and without germinal centers. Based on these distinctions, the TLSs were divided into the following three categories: TLS-negative (tumors without intratumor TLSs), early TLSs (tumors with only lymphocyte aggregates), and mature TLSs (tumors containing at least one lymphoid follicle, with or without germinal centers). Mature TLSs were further subdivided into primary TLSs, which lack germinal centers, and secondary TLSs, which contain germinal centers. Since early TLSs lack a typical structure and their functional significance remains unclear, only mature primary and secondary TLSs were included in the scoring model.

To evaluate the spatial distribution of the TLSs, each H&E-stained tissue section was divided into two subregions: T and P. The arrangement and abundance of TLS in these subregions were noted. Based on these observations, a TLS scoring system was developed to quantify these characteristics in both regions. Under the system, the T score, which represents T TLS richness, was graded on a four-point scale as follows: 0 points: no TLSs in the T zone; 1 point: 1 or 2 TLSs in the T zone; 2 points: at least 3 TLSs in the T zone, but not enough to meet the threshold of 3 points; and 3 points: a large number of TLSs distributed in the T zone, forming a convergent structure. Similarly, the P score, which represents P TLS abundance, was graded on a four-point scale as follows: 0 points: no typical TLSs in the P region; 1 point: TLSs distributed in less than 50% of the P region; 2 points: TLSs distributed in more than 50% of the P region; and 3 points: a large number of TLSs distributed throughout the P region, converging with each other.

Notably, while the TLSs at different stages of maturation were included in the evaluation, the granulocytes in the necrotic areas were excluded from the scoring process. For further details on the scoring methods of the TLS scoring system (which comprises the T score and P score), see Table S1.

Animal model and FOLFOX treatment

To investigate the effect of FOLFOX chemotherapy on TLS formation in CC, a mouse subcutaneous transplant tumor model was established. Six-week-old male C57BL/6 mice (weighing 18–22 g, n=24), purchased from Nanjing YK Biotech Co., Ltd. (Nanjing, China) were used for this experiment. All mice underwent a 7-day immunological acclimatization and observation period before tumor cell injection. The animals were housed in individually ventilated cages under specific pathogen-free (SPF) conditions, with a 12-hour light/dark cycle, constant temperature (22±2 ℃), and relative humidity (50%±10%), and had free access to autoclaved food and water. Animal experiments were approved by the Animal Ethics Committee of Harbin Medical University Cancer Hospital (approval No. KY2016-23), in compliance with institutional guidelines for the care and use of animals.

Mouse CC cells (MC38) were cultured under standard conditions, and subcutaneously injected [5×10^5 cells in 100 µL phosphate buffered saline (PBS)] into the right flank of each mouse. Tumor growth was monitored daily, and once the tumors reached approximately 100 mm^3 (14–21 days post-injection), the mice were randomized into the following two groups: the control group (n=10); and the FOLFOX treatment group (n=10). The mice in the FOLFOX group received intraperitoneal (i.p.) injections of the following drugs twice a week for 2 weeks: folinic acid (25 mg/kg), oxaliplatin (5 mg/kg) and 5-fluorouracil (50 mg/kg). The mice in the control group received i.p. injections of equivalent volumes of PBS under the same

schedule. All animals were housed in the same facility under identical environmental conditions, and the order of treatment administration was balanced across groups to minimize potential confounding factors such as cage location or treatment sequence. Animals were monitored daily for signs of pain, distress, or adverse effects such as weight loss >20%, ulceration, or abnormal behavior, and were euthanized according to institutional guidelines if these limits were exceeded or if tumor size reached >1,500 mm^3. The group allocation was based on a pre-defined randomization sequence, and the full allocation is provided in Table S2.

Histological analysis of TLS formation

After the treatment period, the tumors were harvested, fixed in formalin, and embedded in paraffin for histological examination. H&E staining was performed to assess tumor morphology and TLS formation. TLS presence and size were analyzed in both the control and FOLFOX-treated groups by calculating the TLS area relative to the tumor area.

Flow cytometry analysis of immune cell infiltration

To quantify the immune cell infiltration in the tumor, spleen, and lymph nodes, single-cell suspensions were prepared by mechanical dissociation followed by filtration through a 70 μm cell strainer. The cells were stained with fluorescently labeled antibodies for immune markers including CD19/CD45 (B cells), CD80/CD86 (DCs), CD4 (helper T cells), and CD8 (cytotoxic T cells). Flow cytometry was conducted using a FACScanto II flow cytometer (BD Biosciences, Franklin Lakes, NJ, USA), and the data were analyzed using FlowJo software (FlowJo, Canada).

Statistical analysis

All statistical analyses were performed using SPSS version 22.0 (SPSS Inc., USA) and R version 3.6.3 (R Foundation for Statistical Computing, Vienna, Austria). The normality of continuous variables was assessed using the Shapiro-Wilk test. For normally distributed data, independent-samples *t*-tests were used to compare differences between groups, such as between control and FOLFOX-treated groups in the animal experiments. For non-normally distributed variables, the Mann-Whitney *U* test was applied. Categorical variables were compared using Pearson's χ^2 test or Fisher's exact test, as appropriate. To assess the modulatory effect of FOLFOX chemotherapy on TLS formation, the presence and area of TLSs, as well as the proportions of immune cell subsets ($CD4^+$, $CD8^+$ T cells, $CD19^+$ B cells, and $CD80^+CD86^+$ dendritic cells), were compared between drug-treated and control mice using *t*-tests or non-parametric tests, depending on data distribution. These analyses aimed to determine whether TLSs were induced or enhanced by chemotherapy *in vivo*. In survival analysis, the Kaplan-Meier method was used to estimate OS, and differences between groups—such as TLS-positive *vs.* TLS-negative patients, or patients stratified by T score and P score—were assessed using the log-rank test. The Cox proportional hazards regression model was applied for multivariate analysis to identify independent prognostic factors. The Harrell's concordance index (C-index) was used to evaluate the predictive performance of the TLS scoring systems. A C-index value >0.70 was considered indicative of a model with good discriminative ability. For statistical analysis in animal experiments, at least three mice per group were included. A two-sided P value <0.05 was considered statistically significant.

Results

Clinicopathologic characteristics

The clinicopathological characteristics of the two patient cohorts are summarized in *Tables 1,2*. Cohort 1 (*Table 1*) comprised 374 patients with an average age of 59.79 years (range, 20–86 years), of whom, 211 were male (56.4%) and 163 were female (43.6%). In Cohort 1, the majority of tumors were located in the right colon (155 cases, 41.4%), and the distribution of TNM stages was as follows: stage II (209 patients, 55.9%), stage III (148 patients, 39.6%), and stage IV (17 patients, 4.5%). Cohort 2 (*Table 2*) comprised 239 CC patients with an average age of 67.53 years (range, 31–90 years) and an equal distribution of males (53.1%) and females (46.8%). In Cohort 2, the distribution of TNM stages I, II, III, and IV were 15.0%, 37.6%, 28.8%, and 14.6%, respectively. Collectively, the clinicopathologic characteristics provide a comprehensive overview of the patient cohorts, establishing a foundation for the subsequent analyses of the TLS distribution and immune characteristics of CC.

Table 1 Clinical characteristics of patients in the Harbin Medical University cohort

Characteristics	Value
Sex	
Male	211 (56.4)
Female	163 (43.6)
Age (years)	59.79±11.46
Lymphocyte counts (cells/μL)	7.17±2.29
Percentage of mononuclear cells (%)	7.13±2.43
Absolute value of mononuclear cells (cells/μL)	0.50±0.22
Percentage of lymphocytes (%)	28.56±9.69
Absolute value of lymphocyte (cells/μL)	1.98±0.91
Percentage of basophils (%)	0.54±0.40
Absolute value of basophils (cells/μL)	0.24±3.90
Percentage of eosinophils (%)	2.65±9.74
Absolute value of eosinophils (cells/μL)	0.15±0.11
Percentage of neutrophils (%)	61.63±10.51
Absolute value of neutrophils (cells/μL)	4.54±2.08
Carcinoembryonic antigen (ng/mL)	10.37±22.66
Carbohydrate antigen-199 (ng/mL)	28.30±55.47
Tumor location	
Transverse colon	32 (8.6)
Appendix	19 (5.1)
Sigmoid colon	144 (38.5)
Right hemicolon	155 (41.4)
Descending colon	24 (6.4)
Tumor size (mm^2)	159.25±534.24
Broad types	
Infiltrating ulcer type	78 (20.9)
Infiltrating type	43 (11.5)
Ulcerative type	16 (4.3)
Flaring type	237 (63.4)
Tumor differentiation	
Undifferentiated	26 (7.0)
Well differentiated	19 (5.1)
Moderately differentiate	295 (78.9)
Poorly differentiated	34 (9.1)
Histological type	
Mucious adenocarcinoma	28 (7.5)
Adenocarcinoma	344 (92.5)
MMR	
dMMR	62 (16.6)
pMMR	302 (80.7)
With mucus/Indian ring	119 (31.8)
Neurological invasion	68 (18.2)
Lympho-vascular invasion	35 (9.4)
Pathologic T stage	
2	7 (1.9)
3	213 (57.0)
4	154 (41.2)
Pathologic N stage	
0	207 (55.3)
1	119 (31.8)
2	48 (12.8)
TNM stage	
II	209 (55.9)
III	148 (39.6)
IV	17 (4.5)
Presence of TLS	
Yes	202 (54.0)
No	172 (46.0)

Data are presented as mean ± standard deviation or n (%). dMMR, deficient mismatch repair; MMR, mismatch repair; pMMR, proficient mismatch repair; TNM, Tumor-Node-Metastasis; TLS, tertiary lymphoid structure.

TIME composition of CC

The tumor immune microenvironment (TIME) plays a crucial role in CC development (26,27). An immune infiltration analysis of the CC tissue and adjacent normal colon tissue from TCGA-COAD CC cohort showed significant differences in the immune cell composition between normal and tumor tissue (*Figure 1A*). Notably, the tumor tissue was enriched in B cells, T cells, monocyte

Table 2 Clinical characteristics of patients in TCGA-COAD external validation cohort

Characteristics	Value
Sex	
Male	127 (53.1)
Female	112 (46.8)
Age (years)	67.53±12.45
Pathologic T stage	
1	7 (2.9)
2	38 (15.8)
3	165 (69.0)
4	29 (12.1)
Pathologic N stage	
0	137 (57.3)
1	52 (21.7)
2	50 (20.9)
Pathologic M stage	
0	209 (84.1)
1	35 (14.6)
TNM stage	
I	36 (15.0)
II	90 (37.6)
III	69 (28.8)
IV	35 (14.6)
Presence of TLS	
Yes	120 (50.2)
No	119 (49.8)

Data are presented as mean ± standard deviation or n (%). TCGA-COAD, The Cancer Genome Atlas Colon Adenocarcinoma; TLS, tertiary lymphoid structure; TNM, Tumor-Node-Metastasis.

lineage, and cytotoxic lymphocytes, suggesting the presence of TLSs. In addition, chemokines were differentially expressed between tissues, further supporting the association between TLSs and immune infiltration (*Figure 1B*). IHC staining using CD45 as a marker for lymphocytes showed significant immune cell infiltration in the tumor tissue compared to the normal tissue, highlighting the immune-specific environment tailored to TLSs in CC (*Figure 1C*). Together, the immune cell composition and chemokine differences in the CC tissue suggest a unique TIME that may facilitate TLS formation.

Characteristics and maturation of TLSs in CC

The TLSs were identified in the tumor stroma and at the periphery of the tumor tissue. No TLSs were observed in the adjacent normal colon tissue. TLSs varied in size and shape, such that the majority were oval, fusiform, or irregular (*Figure 2*). In the two cohorts, TLSs were detected in 54.0% and 50.2% of the samples, respectively. H&E and IHC staining confirmed that TLSs consisted of a $CD3^+$ T cell area and a $CD20^+$ B cell area, and that B cell follicles comprised the main component of TLSs (*Figure 2A*). Furthermore, the mIHC analysis showed that the TLSs had an accumulation of $CD4^+$ T cells, $CD8^+$ T cells, $CD20^+$ B cells, $CD21^+$ DCs, and $CD23^+$ FDCs (*Figure 2B-2D*). The quantification of immune cells in the TLSs showed that $CD8^+$ T cells were the most abundant (36.16%), followed by $CD20^+$ B cells (26.21%), $CD4^+$ T cells (24.67%), $CD21^+$ DCs (9.93%), and $CD23^+$ FDCs (3.03%) (*Figure 2E,2F*).

TLSs undergo several stages of maturation, progressing. Early TLSs to primary TLSs, and eventually to secondary TLSs. The early TLSs comprised lymphocyte aggregates with fewer than 50 lymphocytes. Primary TLSs had a regular morphology, with $CD3^+$ T cells surrounding $CD20^+$ B cells, while secondary TLSs formed germinal centers with dense clusters of T cells around B cell follicles (*Figure 3A-3C*). Additionally, TLSs were observed in both the T and P regions of the CC tissue (*Figure 3D*).

These findings showed that TLSs in the CC tissues exhibited distinct maturation stages and cellular compositions, which might play a significant role in modulating the tumor immune environment and influencing tumor progression.

Correlation between the presence of TLSs and OS in CC

We explored the association between the presence of TLSs and OS in both cohorts. The Kaplan-Meier survival analysis showed that the TLS-positive patients had significantly better survival than the TLS-negative patients. In Cohort 1, the TLS-positive patients had a higher survival rate (χ^2=51.053, P<0.001), and similar results were observed in Cohort 2 (χ^2=22.993, P<0.001) (*Figure 4*). Thus, the presence of TLSs was found to be a positive prognostic marker in CC, and correlated with prolonged OS.

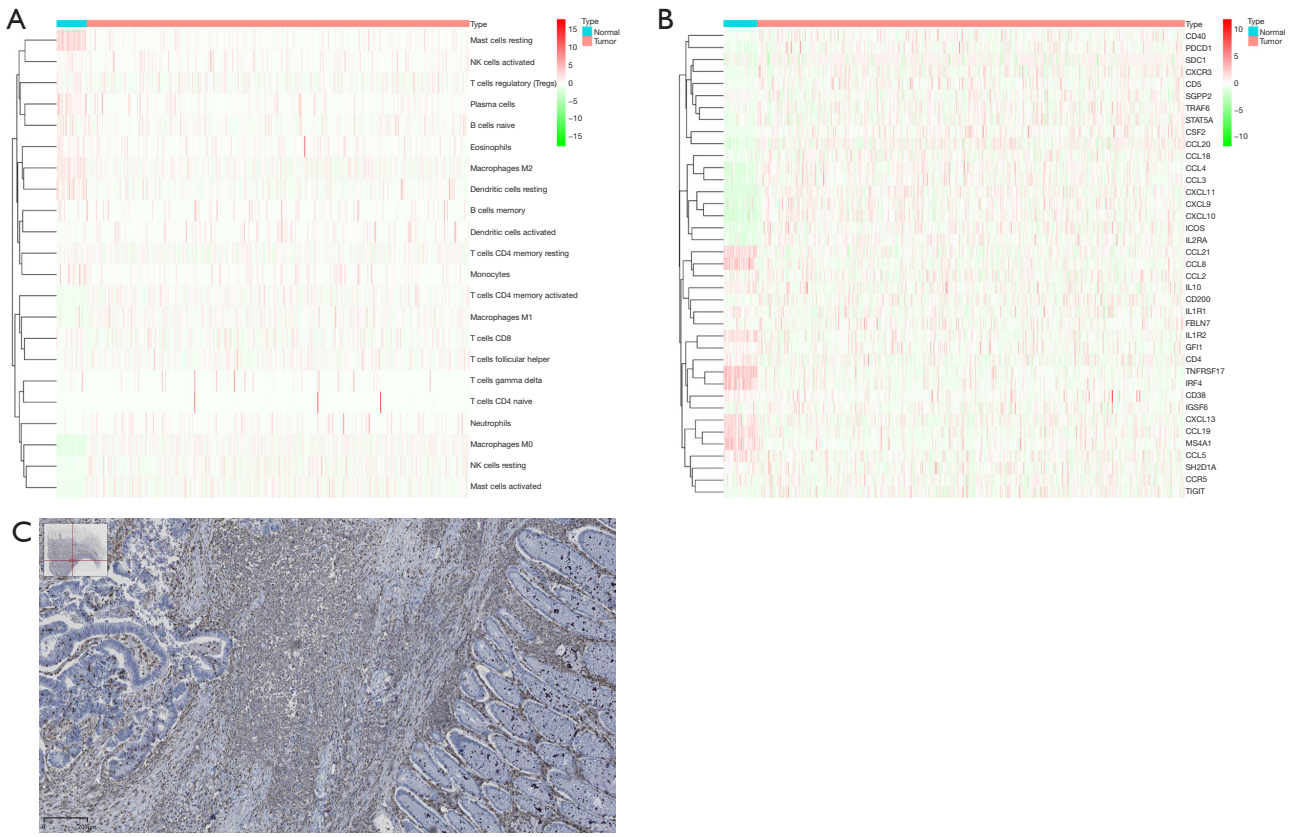

Figure 1 Analysis of the TIME in normal and CC tissues. (A) Heatmap showing the composition of the immune cell types in the TIME of the normal colon versus CC tissues. (B) Heatmap displaying the differential expression of chemokines between the normal colon and CC tissues. (C) IHC staining for $CD45^{+}$ lymphocytes in the CC tissue sections, indicating immune cell infiltration. Scale bar: 50 μm and 200 μm. CC, colorectal cancer; IHC, immunohistochemistry; TIME, tumor immune microenvironment.

Cox regression analysis of prognostic mortality in CC patients

To further investigate the prognostic factors affecting the mortality of CC patients, we conducted a multivariate Cox regression analysis incorporating variables such as perineural invasion, TLS status, tumor type, differentiation grade, T score, and P score to predict the 3-, 5-, and 10-year survival rates of the patients (*Table 3*). The results showed that perineural invasion was associated with a higher mortality risk, while TLS positivity was correlated with improved survival. Patients with the "infiltrative type", moderate differentiation, and higher P scores had an elevated risk of death, while higher T scores were linked to reduced mortality. The nomogram model had high predictive accuracy, particularly for 3-year survival (area under the curve: 0.811, *Figure 5*).

To assess whether TLS was an independent prognostic factor, three Cox models were constructed: (I) a pathological model that included broad tumor types, neurological invasion, CEA, carbohydrate antigen-199, and TNM stage; (II) a molecular model, which comprised the pathological model plus mismatch repair (MMR) protein status; and (III) a molecular-immune model, which comprised the molecular model plus TLS status. The molecular-immune model achieved the highest predictive accuracy, with a C-index of 0.774 (95% CI: 0.727, 0.821) (P<0.001), outperforming the pathological and molecular models (Figure S1, Table S3).

Thus, TLS positivity was found to be an independent protective factor and a strong predictor of survival in CC. These findings suggest that it could serve as a potential indicator of patient prognosis.

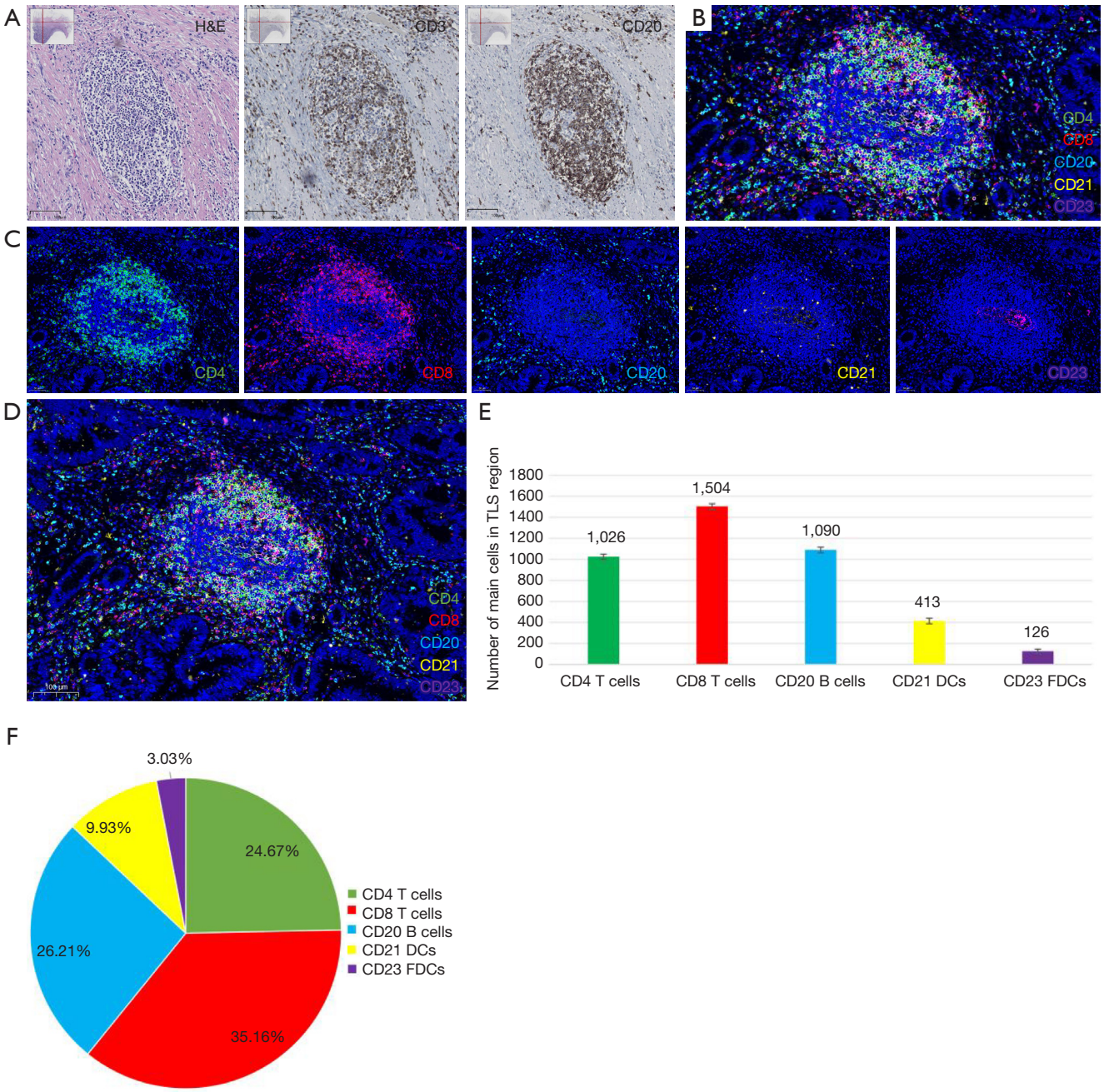

Figure 2 Distribution and composition of TLSs in CC tissue. (A) H&E and IHC staining showing that the TLSs primarily comprise a CD3$^+$ T cell zone and a CD20$^+$ B cell area, with B cell follicles as the main component of TLS. Scale bar: 20 μm, 100 μm. (B) mIHC staining showing the accumulation of CD4$^+$ T cells (green), CD8$^+$ T cells (red), CD20$^+$ B cells (blue), CD21$^+$ DCs (yellow), and CD23$^+$ FDCs (purple) in TLSs. Scale bar: 100 μm. (C) mIHC images with individual markers showing the distribution of CD4, CD8, CD20, CD21, and CD23 cells in TLSs. Scale bar: 50 μm. (D) mIHC image with combined markers showing the colocalization of multiple cell types in TLSs. Scale bar: 100 μm. (E) Histogram depicting the distribution of main immune cell populations in the TLS region. (F) Pie chart showing the proportion of main immune cell populations in TLSs. CC, colorectal cancer; DCs, dendritic cells; FDCs, follicular dendritic cells; H&E, hematoxylin and eosin; IHC, immunohistochemistry; mIHC, multispectral immunohistochemistry; TLS, tertiary lymphoid structure.

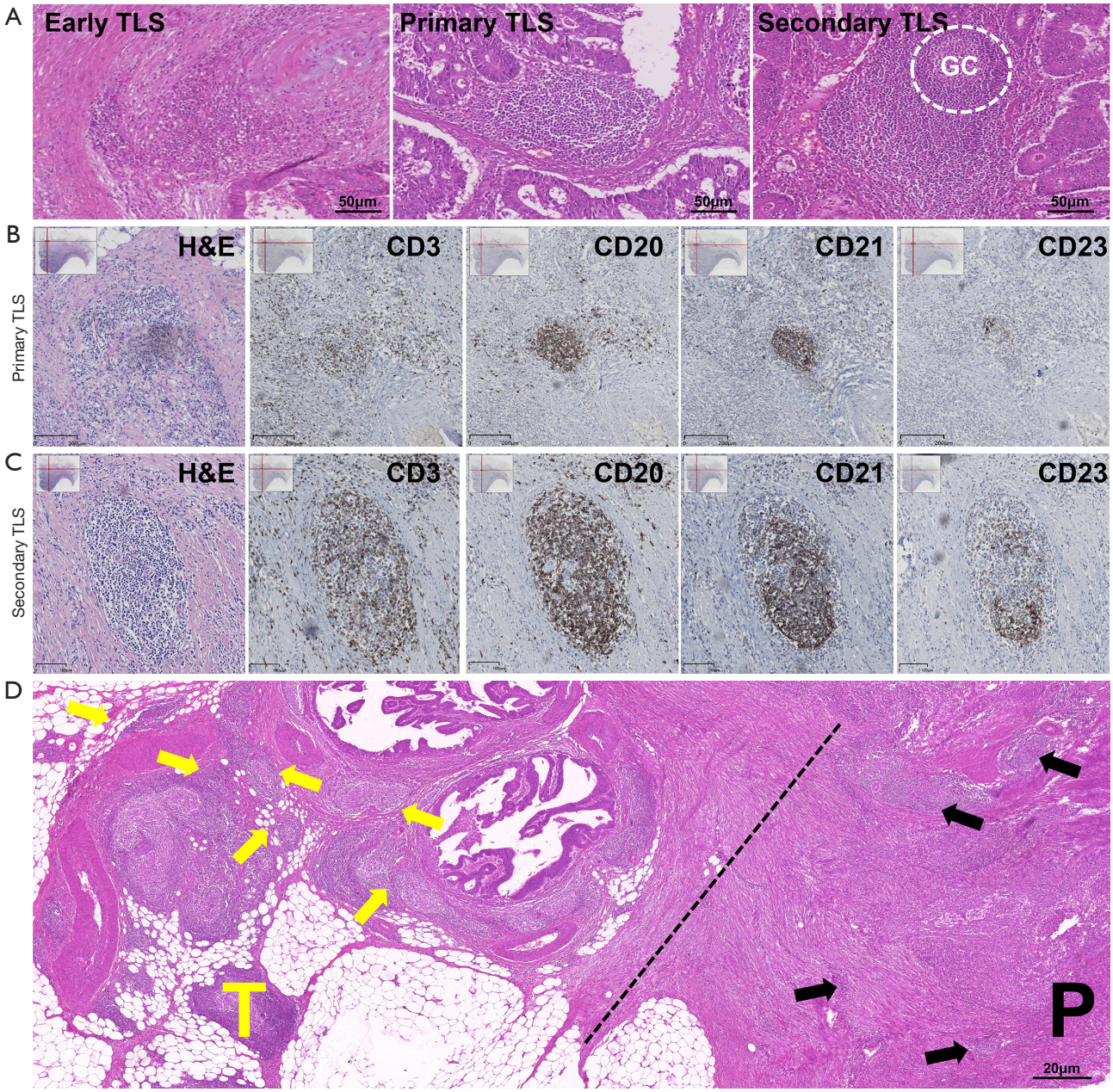

Figure 3 Maturation stages of TLSs in CC tissue. (A) H&E staining showing the three maturation stages of TLSs: early TLSs, primary TLSs, and secondary TLSs. Secondary TLSs exhibit distinct GCs. Scale bar: 50 μm. (B,C) IHC staining of primary and secondary TLSs showing the structural organization, with $CD3^+$ T cells surrounding $CD20^+$ B cells; secondary TLSs form GCs with dense T cell clusters around B cell follicles. Scale bar: 20 μm, 100 μm, 200 μm. (D) H&E staining showing the distribution of TLSs in the T and P regions, with yellow arrows indicating the locations of TLSs, and a dashed line marking the boundary between the intratumoral and P areas, the black arrows indicate the peripheral region of the tumor (P region). Scale bar: 20 μm. CC, colorectal cancer; GCs, germinal centers; H&E, hematoxylin and eosin; IHC, immunohistochemistry; T, intratumoral; P, peritumoral; TLS, tertiary lymphoid structure.

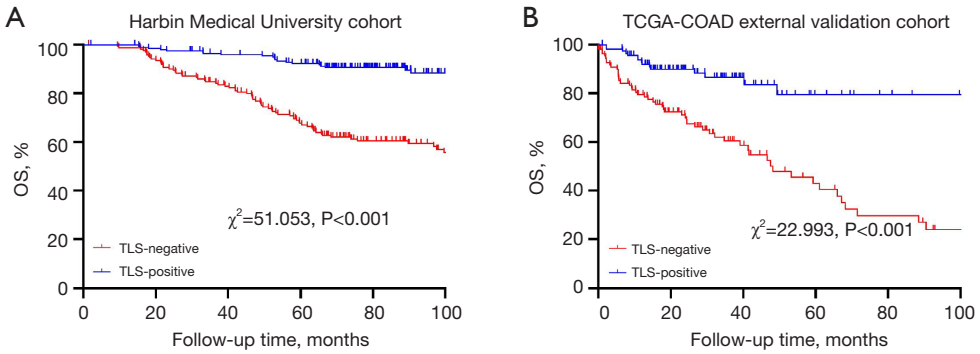

Figure 4 Kaplan-Meier curves illustrating OS based on TLS status in the CC patients from the two cohorts. (A) OS comparison between the TLS-positive and TLS-negative patients in the Harbin Medical University cohort. (B) OS comparison between the TLS-positive and TLS-negative patients in TCGA-COAD external validation cohort. CC, colorectal cancer; OS, overall survival; TLS, tertiary lymphoid structure; TCGA-COAD, The Cancer Genome Atlas Colon Adenocarcinoma.

TLSs in different subregions and prognostic implications

We further analyzed the prognostic significance of TLS distribution in the T and P regions using the T and P score. The Kaplan-Meier survival curves revealed that higher T scores were associated with a lower mortality risk, while higher P scores were associated with a worse prognosis. In both cohorts, the patients with higher T scores (T2 group) had better survival outcomes (Cohort 1: χ^2=18.299, P<0.001; Cohort 2: χ^2=13.653, P=0.003). Conversely, in both cohorts, the patients with lower T scores had a higher mortality risk (Cohort 1: χ^2=6.619, P=0.045; Cohort 2: χ^2=21.826, P<0.001) (*Figure 6*).

These results suggested that TLS distribution in different regions of CC tissues had distinct prognostic implications, such that higher T scores were linked to better outcomes, and higher P scores were linked to poorer outcomes.

Effect of FOLFOX treatment on TLS formation in a mouse model

To explore whether FOLFOX treatment) affected TLS formation, a mouse subcutaneous transplant tumor model was established. The histological analysis showed that the TLS formation in the FOLFOX-treated tumors resembled human TLS. The incidence and size of TLS was increased in the FOLFOX treatment group compared to the control group (*Figure 7A-7C*). Flow cytometry of the tumor, spleen, and lymph node samples from both groups revealed that FOLFOX significantly increased the infiltration of B cells, T cells, and DC cells, which are key components of TLSs (*Figure 7D-7F*). These results suggested that FOLFOX promoted TLS formation and enhanced immune cell infiltration.

Discussion

This study conducted a comprehensive evaluation of TLSs in stage III CC, examining their composition, maturation stages, spatial distribution, and prognostic significance. Our findings offer new insights into the TIME in stage III CC, highlighting TLSs as a crucial component that modulate the immune response and influence patient outcomes.

TLSs were identified as major immune aggregates in the tumor stroma and at the periphery of the CC tissue, and were absent in the adjacent normal tissue. This spatial specificity emphasizes the tumor-related nature of TLSs. The IHC and mIHC analyses revealed that TLSs in CC contain $CD8^+$ T cells, $CD20^+$ B cells, $CD4^+$ T cells, DCs, and FDCs, which is consistent with previous findings for other malignancies (28). The hierarchical organization of immune cells in TLSs reflects their functional maturity, such that mature TLSs exhibit enhanced immunogenicity due to germinal center formation. This aligns with previous reports that suggest that mature TLSs are key promoters of anti-tumor immunity (15,29). Our study also showed that TLS-positive patients had significantly better OS than TLS-negative patients in both the Harbin Medical University cohort and TCGA-COAD external validation cohort, confirming that TLSs are an independent prognostic factor in stage III CC, and supporting the association between TLS density and improved OS in other

Table 3 Univariate and multivariate Cox regression analyses of overall survival

Characteristics	Univariate analysis		Multivariate analysis	
	P	HR (95% CI)	P	HR (95% CI)
Percentage of mononuclear cells	0.02	1.086 (1.016–1.160)	0.13	1.130 (0.964–1.325)
Absolute value of mononuclear cells	0.006	3.201 (1.399–7.323)	0.22	2.720 (0.551–13.428)
MMR				
dMMR	0.01	0.591 (0.388–0.900)	0.41	1.370 (0.649–2.894)
Neurological invasion				
Yes	0.007	1.888 (1.193–2.987)	0.003	3.252 (1.489–7.101)
TLS				
Yes	<0.001	0.197 (0.093–0.707)	0.009	0.256 (0.093–0.707)
Broad types				
Infiltrating ulcer type	0.17	1.485 (0.895–2.465)	0.23	1.724 (0.705–4.215)
Infiltrating type	0.001	2.384 (1.399–4.063)	0.002	3.167 (1.539–6.517)
Ulcerative type	0.19	1.855 (0.737–4.667)	0.07	4.347 (0.912–20.721)
Tumor differentiation				
Undifferentiated	0.02	3.008 (1.183–7.646)	0.24	0.201 (0.014–2.891)
Low	0.14	2.195 (0.769–6.263)	0.78	0.765 (0.117–4.996)
Moderate	0.92	1.040 (0.477–2.266)	0.04	0.304 (0.096–0.955)
Histological type				
Mucious adenocarcinoma	0.01	2.241 (1.192–4.213)	0.12	5.395 (0.643–45.231)
Pathologic N stage				
N1	0.37	1.242 (0.775–1.990)	0.26	1.576 (0.719–3.457)
N2	0.001	2.425 (1.438–4.092)	0.11	2.104 (0.854–5.186)
T score				
T1	0.008	0.362 (0.171–0.766)	0.008	0.200 (0.061–0.656)
T2	0.003	0.173 (0.054–0.556)	0.23	0.462 (0.131–1.628)
T3	0.17	0.462 (0.091–1.536)	0.97	<0.001
P score				
P1	0.052	1.714 (0.994–2.953)	0.38	0.509 (0.113–2.300)
P2	0.43	1.301 (0.678–2.495)	0.15	1.842 (0.797–4.257)
P3	0.03	1.998 (1.061–3.762)	0.04	5.887 (1.091–31.773)

CI, confidence interval; dMMR, deficient mismatch repair; HR, hazard ratio; MMR, mismatch repair; TLS, tertiary lymphoid structure.

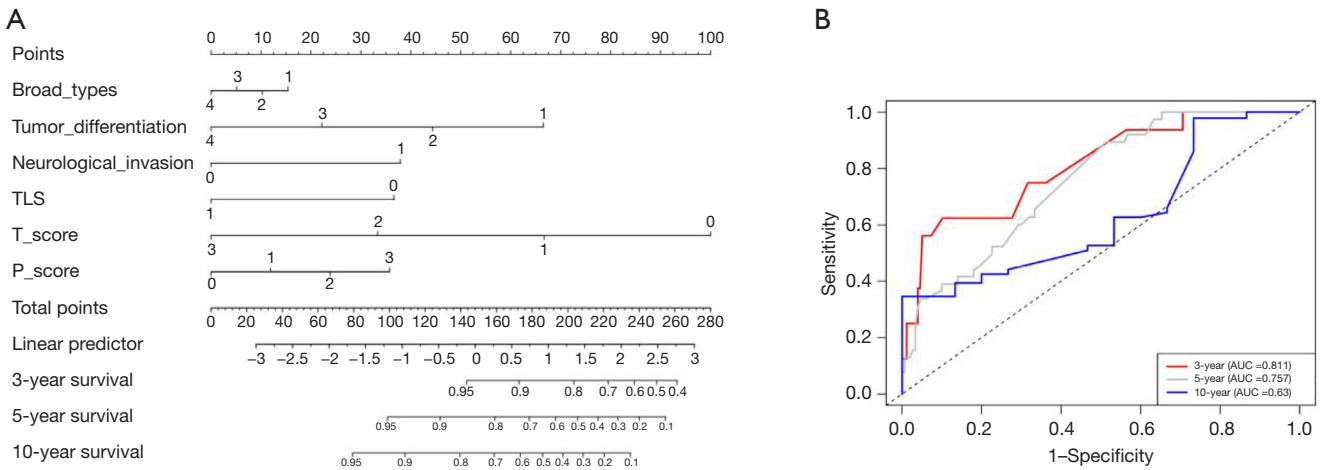

Figure 5 Nomogram for predicting OS in CC patients and its predictive performance. (A) Nomogram incorporating factors such as tumor type, differentiation, neurological invasion, TLS presence, T score, and P score to estimate 3-, 5-, and 10-year OS probabilities. Each predictor is assigned a score, and the total points correlate with the predicted survival rates. Each predictor is assigned a score, and the total points correlate with the predicted survival rates. The numbers represent different categories of each factor, with higher values indicating more severe conditions or worse prognosis. For Broad type, Tumor differentiation, Neurological invasion, and TLS, the scale ranges from 0 to 4, with 0 indicating the best prognosis and 4 representing the worst prognosis. Higher values indicate more severe conditions or worse prognosis. (B) Receiver operating characteristic curves showing the predictive accuracy of the nomogram for 3-, 5-, and 10-year OS. AUC, area under the curve; CC, colorectal cancer; OS, overall survival; TLS, tertiary lymphoid structure.

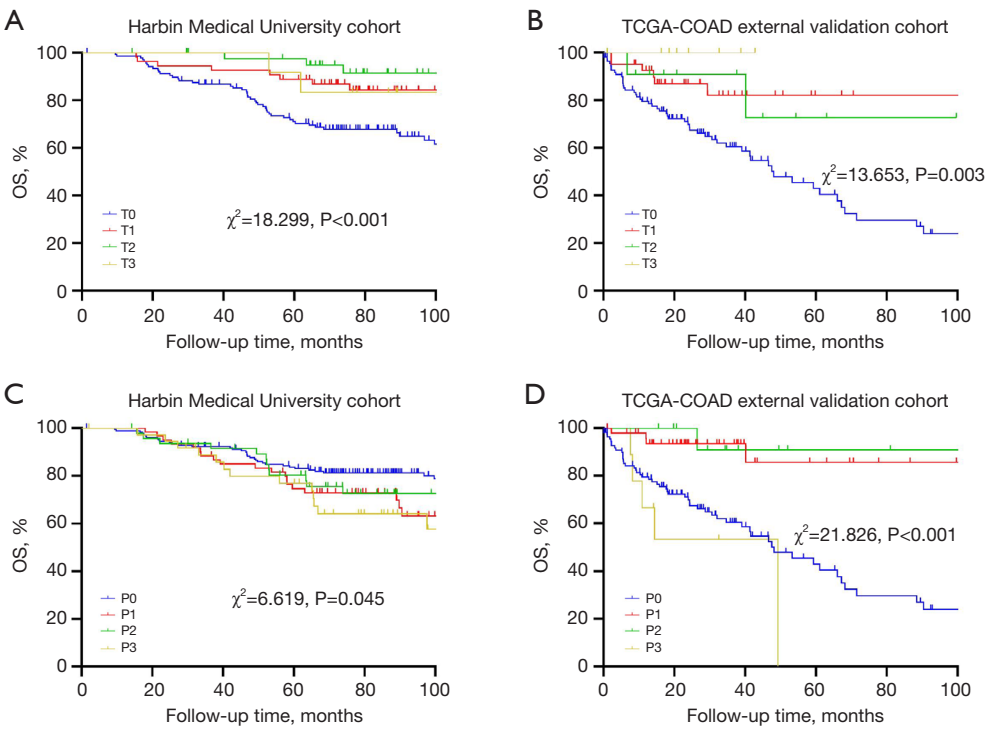

Figure 6 Kaplan-Meier survival curves for OS based on T and P staging in CC patients across two cohorts. (A) OS comparison among T0, T1, T2, and T3 stages in the Harbin Medical University cohort. (B) OS comparison among T0, T1, T2, and T3 stages in TCGA-COAD external validation cohort. (C) OS comparison among P0, P1, P2, and P3 stages in the Harbin Medical University cohort. (D) OS comparison among P0, P1, P2, and P3 stages in TCGA-COAD external validation cohort. CC, colorectal cancer; OS, overall survival; TCGA-COAD, The Cancer Genome Atlas Colon Adenocarcinoma.

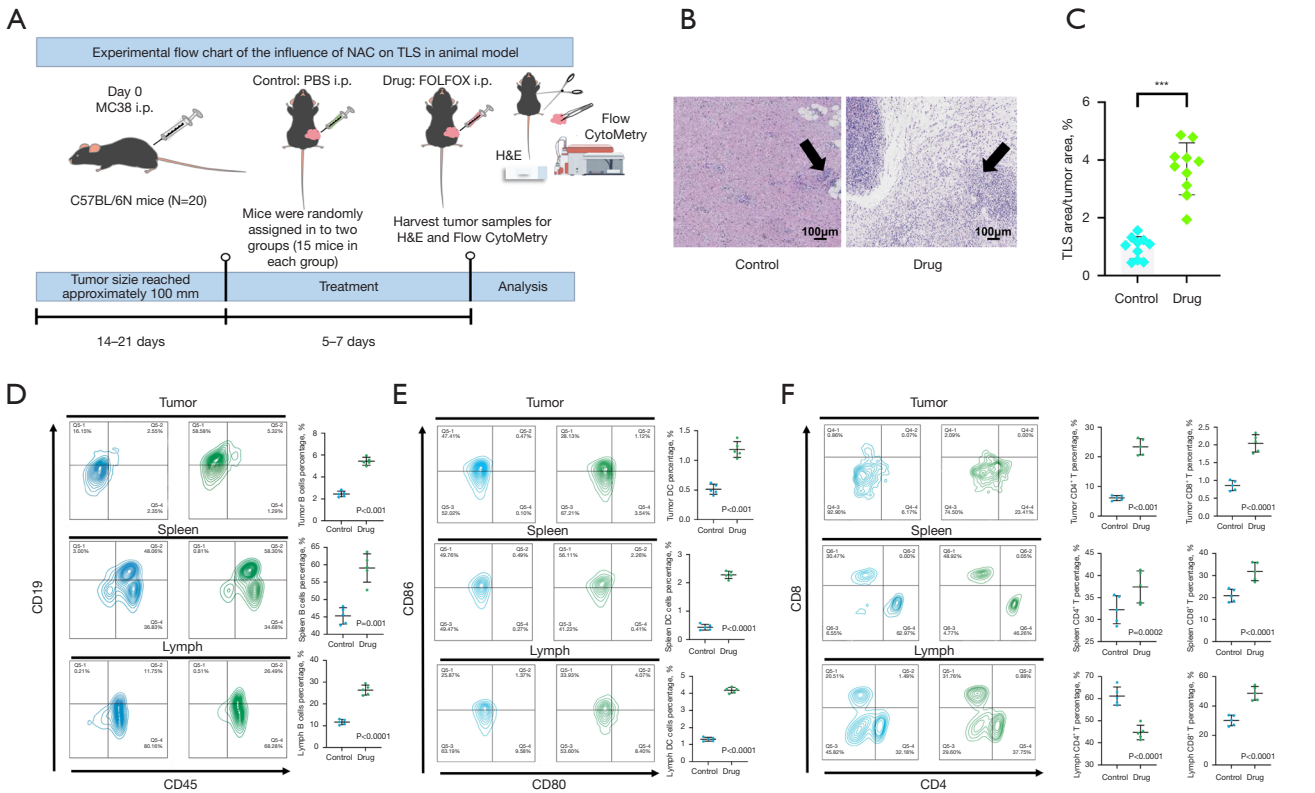

Figure 7 Induction of TLS formation in the tumors of the mice treated with NAC (FOLFOX regimen). (A) Experimental workflow showing the influence of NAC on TLS formation in a mouse tumor model. (B) Representative H&E staining images of TLSs in subcutaneous tumors from the control and FOLFOX-treated mice. Arrows indicate the TLS regions. Scale bar: 100 μm. (C) Quantification of TLS area as a percentage of the tumor region in the control and drug groups (n=10). ***, P<0.001 *vs.* control group. (D-F) Flow cytometry analysis of immune cell populations in the tumor, spleen, and lymph nodes, showing B cells ($CD45^+$ and $CD19^+$), DCs ($CD80^+$ and $CD86^+$), and T cells ($CD4^+$ and $CD8^+$) in the control (left) and drug (right) groups. Statistical significance was determined by *t*-test, as indicated in the figure. DCs, dendritic cells; FOLFOX, folinic acid, oxaliplatin, and 5-fluorouracil; H&E, hematoxylin and eosin; NAC, neoadjuvant chemotherapy; PBS, phosphate buffered saline; TLS, tertiary lymphoid structure.

solid tumors (30). However, the function of TLS and its role in tumor immunity still require further investigation. Specifically, the localization of TLS in the tumor periphery versus interior may impact immune function. Peritumoral TLS may reflect immune surveillance, while intratumoral TLS could indicate immune response failure or immune escape. Future research should explore the contributions of TLS location and immune composition to tumor immunity and prognosis.

An innovative aspect of our study was the development of a TLS scoring system that integrates T and P scores, capturing both TLS abundance and spatial distribution. Our results demonstrated that intratumoral TLSs (T score) are associated with improved prognosis, while peritumoral TLSs (P score) correlate with increased mortality risk. The association between higher P scores and poorer outcomes suggests that P-type TLSs may reflect either a more aggressive tumor phenotype or a failure in initiating an effective anti-tumor immune response, potentially due to the enrichment of immunosuppressive cells such as regulatory T cells. This dual scoring system emphasizes the prognostic relevance of TLS spatial heterogeneity and enhances the utility of TLSs as immune-based prognostic markers in stage III colorectal cancer. Notably, our findings align with recent trends observed across other tumor types. A bibliometric analysis in lung cancer underscored the structural complexity and spatial significance of TLSs in the tumor immune landscape, offering mechanistic insights applicable to colorectal cancer and other solid tumors (31). In parallel, emerging prognostic models based on

metabolic cell death pathways, such as disulfidptosis- and ferroptosis-related genes including *DRD4* and *SLC2A3*, have shown promise in stratifying CC patients (32). Unlike these transcriptome-derived metabolic signatures, our TLS scoring system captures the tissue-level immune architecture, offering a complementary perspective. Together, these immune- and metabolism-based approaches highlight the importance of integrating multi-dimensional markers in future models to achieve more comprehensive and individualized risk prediction.

Additionally, our findings provide novel insights into the effect of FOLFOX on TLS formation. In our mouse model, FOLFOX treatment significantly increased TLS density and immune cell infiltration in tumors, spleens, and lymph nodes, suggesting that chemotherapy not only exerts cytotoxic effects but also modulates the TIME by enhancing TLS-associated immune responses (33). This dual action of FOLFOX opens avenues for its potential use in combination with immunotherapies, which could be especially relevant for stage III CC where effective adjuvant treatments are crucial for improving survival outcomes. However, it is important to consider the potential confounding effect of MMR status, as deficient MMR (dMMR) and proficient MMR (pMMR) tumors can exhibit distinct tumor biology and immune responses. MMR status may influence both TLS formation and the effectiveness of immunotherapy, which could impact the observed outcomes. Further studies should take MMR status into account to better understand its role in the efficacy of FOLFOX and immunotherapy combinations in CC treatment.

Additionally, while we observed that FOLFOX promotes TLS formation, the underlying molecular mechanisms remain unclear. It is plausible that FOLFOX activates specific immune signaling pathways, such as the stimulator of interferon genes (*STING*) or nuclear factor kappa-light-chain-enhancer of activated B cells (NF-κB) pathways (34,35), which may facilitate TLS development and function. Future research needs to be conducted to elucidate these pathways, as understanding how chemotherapy influences TLS maturation and immune activation could lead to the development of new therapeutic strategies. By exploring these mechanisms, future studies could identify novel combination therapies that leverage TLSs to enhance the efficacy of immunotherapies specifically in stage III CC.

Although this study used visual assessment for TLS scoring, future research could consider incorporating automated image analysis tools, such as AI-based TLS detection, to improve the reproducibility and consistency of results. Utilizing automated software like ImageJ or QuPath, combined with deep learning techniques such as convolutional neural networks, can significantly reduce inter-observer variability and enhance the efficiency and accuracy of the scoring system. This improvement would not only increase the reproducibility of results but also facilitate the translational application of the TLS scoring system in clinical settings.

In conclusion, this study highlights TLS as a significant prognostic marker in stage III CC and underscores the potential of FOLFOX chemotherapy in regulating the TIME through TLS formation. Future research should validate these findings in clinically relevant models, investigate the molecular mechanisms of chemotherapy-induced TLS formation, and explore TLS's role in personalized treatment strategies for stage III CC. This could lead to more personalized and effective treatments, improving patient prognosis. Although TLS has been established as a prognostic marker, its practical application in clinical decision-making requires further exploration. TLS scoring could help identify patients who would benefit from adjuvant chemotherapy by reflecting the tumor's immune microenvironment. Additionally, TLS scoring has potential as a predictive biomarker for immunotherapy, helping to select patients likely to benefit from treatment.

Limitations

This study provides valuable insights into the prognostic role of TLSs in stage III CC and their modulation by FOLFOX chemotherapy. However, several limitations exist. The retrospective design may introduce bias, and findings may not be universally applicable. The use of a mouse model, while useful, does not fully replicate human tumor microenvironment complexities, and future studies with orthotopic or genetically engineered models could provide more accurate insights. Additionally, while TLS formation and its prognostic value were explored, the underlying molecular mechanisms remain unclear and require further investigation. The small sample size in the external validation cohort (n=69) and the reliance on manual IHC for TLS quantification may limit generalizability and reproducibility. Future work should focus on refining TLS quantification methods to enhance consistency.

Conclusions

This study showed that TLSs are significant prognostic

markers in stage III CC, the presence of TLSs is correlated with improved OS, and FOLFOX chemotherapy enhances TLS formation, potentially modulating the TIME to improve treatment outcomes. These findings support the integration of TLS analysis into personalized CC treatment strategies to guide prognosis and inform tailored therapies. Future research should focus on refining TLS quantification methods, investigating the molecular mechanisms of TLS formation and interaction with FOLFOX, and conducting clinical trials to validate TLS as a predictive biomarker, ultimately advancing personalized therapeutic approaches in CC.

Acknowledgments

None.

Footnote

Reporting Checklist: The authors have completed the ARRIVE and STROBE reporting checklists. Available at https://jgo.amegroups.com/article/view/10.21037/jgo-2025-181/rc

Data Sharing Statement: Available at https://jgo.amegroups.com/article/view/10.21037/jgo-2025-181/dss

Peer Review File: Available at https://jgo.amegroups.com/article/view/10.21037/jgo-2025-181/prf

Funding: This study was supported by funding from the Nn10 Program of Harbin Medical University Cancer Hospital (No. Nn102017-02).

Conflicts of Interest: All authors have completed the ICMJE uniform disclosure form (available at https://jgo.amegroups.com/article/view/10.21037/jgo-2025-181/coif). N.Z.T. receives honorarium from Johnson and Johnson, Medtronic Asia and Device Technologies Asia for proctoring and lectures given. The other authors have no conflicts of interest to declare.

Ethical Statement: The authors are accountable for all aspects of the work in ensuring that questions related to the accuracy or integrity of any part of the work are appropriately investigated and resolved. This study was conducted in accordance with the Declaration of Helsinki and its subsequent amendments, and was approved by the Ethics Committee of the Harbin Medical University Cancer Hospital (Approval No. HMUIRB2024014). Written informed consent was obtained from all participants. Animal experiments were approved by the Animal Ethics Committee of Harbin Medical University Cancer Hospital (Approval No. KY2016-23), in compliance with institutional guidelines for the care and use of animals.

References

1. Luo YH, Yan ZC, Liu JY, et al. Association of tumor budding with clinicopathological features and prognostic value in stage III-IV colorectal cancer. World J Gastroenterol 2024;30:158-69.
2. Morgan E, Arnold M, Gini A, et al. Global burden of colorectal cancer in 2020 and 2040: incidence and mortality estimates from GLOBOCAN. Gut 2023;72:338-44.
3. Li N, Lu B, Luo C, et al. Incidence, mortality, survival, risk factor and screening of colorectal cancer: A comparison among China, Europe, and northern America. Cancer Lett 2021;522:255-68.
4. Hossain MS, Karuniawati H, Jairoun AA, et al. Colorectal Cancer: A Review of Carcinogenesis, Global Epidemiology, Current Challenges, Risk Factors, Preventive and Treatment Strategies. Cancers (Basel) 2022;14:1732.
5. Bos AC, van Erning FN, van Gestel YR, et al. Timing of adjuvant chemotherapy and its relation to survival among patients with stage III colon cancer. Eur J Cancer 2015;51:2553-61.
6. André T, de Gramont A, Vernerey D, et al. Adjuvant Fluorouracil, Leucovorin, and Oxaliplatin in Stage II to III Colon Cancer: Updated 10-Year Survival and Outcomes According to BRAF Mutation and Mismatch Repair Status of the MOSAIC Study. J Clin Oncol 2015;33:4176-87.
7. Chen L, Wang Y, Cai C, et al. Machine Learning Predicts Oxaliplatin Benefit in Early Colon Cancer. J Clin Oncol

2024;42:1520-30.
8. Cao W, Zhang X, Li R, et al. Lipid core-shell nanoparticles co-deliver FOLFOX regimen and siPD-L1 for synergistic targeted cancer treatment. J Control Release 2024;368:52-65.
9. Auclin E, Zaanan A, Vernerey D, et al. Subgroups and prognostication in stage III colon cancer: future perspectives for adjuvant therapy. Ann Oncol 2017;28:958-68.
10. Sobrero AF, Puccini A, Shi Q, et al. A new prognostic and predictive tool for shared decision making in stage III colon cancer. Eur J Cancer 2020;138:182-8.
11. Upadhyay S, Dahal S, Bhatt VR, et al. Chemotherapy use in stage III colon cancer: a National Cancer Database analysis. Ther Adv Med Oncol 2015;7:244-51.
12. Jiang W, Wang H, Dong X, et al. Pathomics Signature for Prognosis and Chemotherapy Benefits in Stage III Colon Cancer. JAMA Surg 2024;159:519-28.
13. Moreno V, Salazar R, Gruber SB. The prognostic value of TILs in stage III colon cancer must consider sidedness. Ann Oncol 2022;33:1094-6.
14. Saberzadeh-Ardestani B, Foster NR, Lee HE, et al. Association of tumor-infiltrating lymphocytes with survival depends on primary tumor sidedness in stage III colon cancers (NCCTG N0147) [Alliance]. Ann Oncol 2022;33:1159-67.
15. Teillaud JL, Houel A, Panouillot M, et al. Tertiary lymphoid structures in anticancer immunity. Nat Rev Cancer 2024;24:629-46.
16. Yu J, Gong Y, Huang X, et al. Prognostic and therapeutic potential of gene profiles related to tertiary lymphoid structures in colorectal cancer. PeerJ 2024;12:e18401.
17. Vaghjiani RG, Skitzki JJ. Tertiary Lymphoid Structures as Mediators of Immunotherapy Response. Cancers (Basel) 2022;14:3748.
18. Yang J, Xu J, Liu H, et al. Deep insight into the B-cell associated tertiary lymphoid structure and tumor immunotherapy. Cancer Biol Med 2023;21:125-31.
19. Wang B, Liu J, Han Y, et al. The Presence of Tertiary Lymphoid Structures Provides New Insight Into the Clinicopathological Features and Prognosis of Patients With Breast Cancer. Front Immunol 2022;13:868155.
20. Zhang Y, Liu G, Zeng Q, et al. CCL19-producing fibroblasts promote tertiary lymphoid structure formation enhancing anti-tumor IgG response in colorectal cancer liver metastasis. Cancer Cell 2024;42:1370-1385.e9.
21. Xu Z, Wang Q, Zhang Y, et al. Exploiting tertiary lymphoid structures gene signature to evaluate tumor microenvironment infiltration and immunotherapy response in colorectal cancer. Front Oncol 2024;14:1383096.
22. Zhou Q, Lan L, Wang W, et al. Comprehensive analysis of tertiary lymphoid structures-related genes for prognostic prediction, molecular subtypes and immune infiltration in gastric cancer. Aging (Albany NY) 2023;15:13368-83.
23. Buisseret L, Desmedt C, Garaud S, et al. Reliability of tumor-infiltrating lymphocyte and tertiary lymphoid structure assessment in human breast cancer. Mod Pathol 2017;30:1204-12.
24. Zhang SR, Yao L, Wang WQ, et al. Tumor-Infiltrating Platelets Predict Postsurgical Survival in Patients with Pancreatic Ductal Adenocarcinoma. Ann Surg Oncol 2018;25:3984-93.
25. Mezheyeuski A, Bergsland CH, Backman M, et al. Multispectral imaging for quantitative and compartment-specific immune infiltrates reveals distinct immune profiles that classify lung cancer patients. J Pathol 2018;244:421-31.
26. Binnewies M, Roberts EW, Kersten K, et al. Understanding the tumor immune microenvironment (TIME) for effective therapy. Nat Med 2018;24:541-50.
27. Chen W, Zhou M, Guan B, et al. Tumour-associated macrophage-derived DOCK7-enriched extracellular vesicles drive tumour metastasis in colorectal cancer via the RAC1/ABCA1 axis. Clin Transl Med 2024;14:e1591.
28. Fridman WH, Pagès F, Sautès-Fridman C, et al. The immune contexture in human tumours: impact on clinical outcome. Nat Rev Cancer 2012;12:298-306.
29. Bao X, Lin X, Xie M, et al. Mature tertiary lymphoid structures: important contributors to anti-tumor immune efficacy. Front Immunol 2024;15:1413067.
30. Wang Q, Shen X, An R, et al. Peritumoral tertiary lymphoid structure and tumor stroma percentage predict the prognosis of patients with non-metastatic colorectal cancer. Front Immunol 2022;13:962056.
31. Liu X, Liu H, Huang L, et al. Inflammation, tertiary lymphoid structures, and lung cancer: a bibliometric analysis. Transl Lung Cancer Res 2024;13:2636-48.
32. Yi N, Zhou Y, Di D, et al. Development and validation of a prognostic model based on disulfidptosis-related ferroptosis genes: DRD4 and SLC2A3 as biomarkers for predicting prognosis in colon cancer. Transl Cancer Res 2025;14:159-78.
33. Weng Y, Yuan J, Cui X, et al. The impact of tertiary lymphoid structures on tumor prognosis and the immune microenvironment in non-small cell lung cancer. Sci Rep

2024;14:16246.
34. Chelvanambi M, Fecek RJ, Taylor JL, et al. STING agonist-based treatment promotes vascular normalization and tertiary lymphoid structure formation in the therapeutic melanoma microenvironment. J Immunother Cancer 2021;9:e001906.
35. Noort AR, van Zoest KP, van Baarsen LG, et al. Tertiary Lymphoid Structures in Rheumatoid Arthritis: NF-κB-Inducing Kinase-Positive Endothelial Cells as Central Players. Am J Pathol 2015;185:1935-43.

Cite this article as: Zhang C, Wang SK, Teo NZ, Wei MYK, Hashida H, Yu CF, Liu YL, Cui BB. Prognostic role of tertiary lymphatic structures and their modulation by adjuvant FOLFOX in stage III colon cancer: a retrospective cohort study. J Gastrointest Oncol 2025;16(2):386-403. doi: 10.21037/jgo-2025-181